those responsible for supergene enrichment, may bind to cell walls in large quantities (*15*). Therefore, the collection and concentration of Cu ions seem to have been the most likely function of these putative bacteria in the enrichment process. However, the electron transfer involved in chalcocite enrichment (*16*) also may be catalyzed bacterially (*5*). Data on S isotopes (*17*) and theoretical modeling (*18*) show that the S in supergene chalcocite is inherited from the hypogene sulfides that it replaced. Hence, the bacteria cannot be of the type dedicated to the reduction of sulfate ions (in the descending solutions) to sulfide. Microbial fixation of Cu at active replacement fronts between hypogene sulfides and chalcocite may be a critical kinetic factor in the enrichment process.

Consequently, climatic or hydrologic conditions that favor the proliferation of bacteria may be an important control on the rate and efficiency of supergene enrichment. Indeed, the hyperarid conditions responsible for the mid-Miocene cessation of enrichment in northern Chile–southern Peru (*7*, *19*) may have been inimical to the bacterial activity. Most of the enrichment in northern Chile–southern Peru took place 100 to 300 m beneath the paleosurface (Fig. 1), which is shallow relative to the maximum recorded depth of ~4 km for subterranean microbial activity (*20*).

REFERENCES AND NOTES

1. W. H. Emmons, *The Enrichment of Ore Deposits* (*U.S. Geol. Surv. Bull. 625*, Government Printing Office, Washington, DC, 1917); A. Locke, *Leached Outcrops as Guides to Copper Ore* (Williams and Wilkins, Baltimore, MD, 1926).
2. G. H. Brimhall, C. N. Alpers, A. B. Cunningham, *Econ. Geol.* **80**, 1227 (1985).
3. C. N. Alpers and G. H. Brimhall, *ibid.* **84**, 229 (1989).
4. L. E. Murr, *Miner. Sci. Eng.* **12**, 121 (1980); B. J. Ralph, in *Comprehensive Biotechnology*, C. W. Robinson and J. A. Howell, Eds. (Pergamon, Oxford, 1985), vol. 4, pp. 201–234; S. Bustos, S. Castro, R. Montealegre, *FEMS Microbiol. Rev.* **11**, 231 (1993); R. Montealegre *et al.*, in *Biohydrometallurgical Technologies*, A. E. Torma, J. E. Wey, V. L. Lakshmanan, Eds. (Minerals, Metals, and Materials Society, American Institute of Mining Engineers, New York, 1993), pp. 1–14.
5. M. N. Hughes and R. K. Poole, *Metals and Microorganisms* (Chapman & Hall, London, 1989).
6. J. R. Watterson, *Geology* **20**, 315 (1992); G. Southam and T. J. Beveridge, *Geochim. Cosmochim. Acta* **58**, 4527 (1994). These are morphologic and experimental studies, respectively.
7. R. H. Sillitoe, in *Geology of the Andes and Its Relation to Hydrocarbon and Mineral Resources*, G. E. Ericksen, M. T. Cañas Pinochet, J. A. Reinemund, Eds. (*Earth Science Series Volume 11*, Circum-Pacific Council for Energy and Mineral Resources, Houston, TX, 1990), pp. 285–311.
8. R. Flores V., in *Actas 4th Congreso Geologico Chileno* (Universidad del Norte, Antofagasta, Chile, 1985), vol. 2, pp. 228–249.
9. J. P. Hunt, J. A. Bratt, J. C. Marquardt L., *Min. Eng.* **35**, 636 (1983).
10. L. B. Gustafson and J. P. Hunt, *Econ. Geol.* **70**, 857 (1975).
11. R. L. Folk, *J. Sediment. Petrol.* **63**, 990 (1993).
12. ———, *Géogr. Phys. Quat.* **48**, 233 (1994).
13. T. J. Beveridge and W. S. Fyfe, *Can. J. Earth Sci.* **22**, 1893 (1985); M. D. Mullen *et al.*, *Appl. Environ. Microbiol.* **55**, 3143 (1989); R. J. C. McLean and T. J. Beveridge, in *Microbial Mineral Recovery*, H. L. Ehrlich and C. L. Brierley, Eds. (McGraw-Hill, New York, 1990), pp. 185–222.
14. C. L. Brierley, in *Microbial Mineral Recovery*, H. L. Ehrlich and C. L. Brierley, Eds. (McGraw-Hill, New York, 1990), pp. 303–323.
15. T. J. Beveridge and R. G. E. Murray, *J. Bacteriol.* **127**, 1502 (1976); N. H. Mendelson, *Science* **258**, 1633 (1992).
16. R. L. Andrew, *Miner. Sci. Eng.* **12**, 193 (1980).
17. C. W. Field and L. B. Gustafson, *Econ. Geol.* **71**, 1533 (1976).
18. J. Ague and G. H. Brimhall, *ibid.* **84**, 506 (1989).
19. R. H. Sillitoe, C. Mortimer, A. H. Clark, *Trans. Inst. Min. Metall. B* **77**, 166 (1968); C. N. Alpers and G. H. Brimhall, *Geol. Soc. Am. Bull.* **100**, 1640 (1988); A. H. Clark, R. M. Tosdal, E. Farrar, A. Plazolles V., *Econ. Geol.* **85**, 1604 (1990).
20. K. Pedersen, *Earth-Sci. Rev.* **34**, 243 (1993).

21. Sample collection at Chuquicamata and El Salvador was carried out with the assistance and permission of Codelco-Chile. We thank W. S. Fyfe and J. R. Kyle for manuscript reviews and R. Espejo for discussions.

19 February 1996; accepted 20 March 1996

Oceanic Anoxia and the End Permian Mass Extinction

Paul B. Wignall and Richard J. Twitchett

Data on rocks from Spitsbergen and the equatorial sections of Italy and Slovenia indicate that the world's oceans became anoxic at both low and high paleolatitudes in the Late Permian. Such conditions may have been responsible for the mass extinction at this time. This event affected a wide range of shelf depths and extended into shallow water well above the storm wave base.

The mass extinction at the end of the Permian marks a serious biotic crisis: both the marine and terrestrial biota suffered near annihilation (*1*). The timing and causes of this event have been uncertain: Sequence stratigraphic analysis of numerous sections have shown that the Permian-Triassic (P-Tr) boundary straddles an interval of rapid, global sea-level rise (*2*, *3*). Similarly, an image of a protracted crisis spread over the last few million years of the Permian has been challenged; it may be a considerably more complex event involving an initial extinction separated by a period of radiation in the latest Permian before the wholesale slaughter at the end of the Permian (*4*). The final crisis may have been entirely restricted to the final one million years of the Permian.

The mechanism of the extinction has been much debated. The rapid eruption of the vast Siberian flood basalts was contemporary with the extinction, and the two events have been linked in several ways (*5*). Many boundary sections contain oxygen-restricted facies, which raises the possibility that marine organisms were killed by anoxia (*2*, *6*). In this report, we demonstrate that anoxia occurred in much shallower water than previously recognized and show that sections of the high-latitude Boreal oceans were also affected by the anoxic event.

If anoxic-dysoxic conditions were responsible for the extinction, then several factors need to be demonstrated. (i) The conditions must have been sufficiently widespread (*6*). Most of the evidence for anoxia has come from equatorial and mid-southern paleolatitudes of the Tethyan Ocean. The nature of environmental changes in the high northerly paleolatitudes of the Boreal Ocean has been unclear. (ii) Anoxia must have affected areas of unusually shallow water, the repository for most marine invertebrate diversity. (iii) There must be a propinquitious relation in space and time between extinction and anoxia.

To answer these questions, we conducted a sedimentological and ichnological study of P-Tr boundary sections in Spitsbergen that lay on the margin of the Boreal Ocean and a similar study, combined with geochemical analysis, of the shallow-water, equatorial sections of western Tethys (northern Italy, southern Austria and Slovenia).

The P-Tr boundary in Spitsbergen has traditionally been placed at the contact between the Permian Kapp Starostin Formation, a cherty limestone and shale, and the shale and sandstone of the Vardebukta Formation (Griesbachian and Dienerian stages of the lowermost Triassic). Available biostratigraphic data are poor, and for the Kapp Starostin Formation, the carbon isotope stratigraphy revealed by its constituent brachiopod and coral fauna is the best guide to its latest Permian (Changxingian Stage) age (*7*). The Vardebukta Formation contains sporadic examples of the ammonoid *Otoceras boreale* near its base, and these are joined by the typical Triassic taxa *Ophiceras* and *Claraia* 20 to 30 m above the base (*8*). Defining the position of the base of the Triassic is a

---

Department of Earth Sciences, University of Leeds, Leeds LS2 9JT, UK.

subject of ongoing debate; the ammonoid and conodont records seem to yield different boundaries: most assign it to the base of the *Hindeodus parvus* conodont zone (9). On the basis of ammonoid-conodont correlations elsewhere, the base of the *H. parvus* zone corresponds to a level high in the range of *O. boreale*. In the Kapp Starostin Formation, this correlation would place the P-Tr boundary tens of meters above the formation boundary.

We examined the P-Tr transition at three locations around Isfjord, Spitsbergen: Kapp Starostin, Kapp Wijk, and Sveltihel. All show a similar facies development, and we thus focus on the best exposed section at Kapp Starostin (Fig. 1). The transition from the Kapp Starostin to the Vardebukta Formation is marked by a change from a cherty, silty mudstone to a shale at the base of a 15-m-thick unit that becomes coarser as we move up. Such parasequences typify the Vardebukta Formation. In the basal 80 m of the formation, thin, current-rippled (and occasional hummocky cross-laminated) sandstone appears near the tops of the parasequences, which indicates a distal storm facies typical of an outer shelf setting.

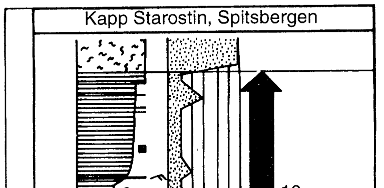

Fig. 1. Sedimentary log and ichnofabric index (II) from the Kapp Starostin section of the P-Tr boundary in western Spitsbergen. Anoxic deposition, characterized by fine lamination, abundant pyrite, and well-preserved fossil fish, began in the latest Permian within a parasequence. This records an event on the margins of the Boreal Ocean at about 50°N. Abbreviations: KSF, Kapp Starostin Formation; HCS, Hummocky cross stratification. Grain size scale: C, clay; Si, silt; and FS, fine sand.

The major paleoenvironmental change in the lower Vardebukta Formation occurs 6 m above the base at a level unrelated to the base-level changes associated with parasequence development. Beneath this level, the mudstones are thoroughly bioturbated by vague sinuous (and occasionally branching) burrows a few millimeters wide [level 6 in the semiquantitative ichnofabric index (II) of Droser and Bottjer (*10*), where 1 indicates no burrowing activity and 6 indicates complete bioturbation]. Above the 6-m level, burrows disappear, the sediments are finely laminated, and framboidal pyrite is common to abundant. Complete, articulated fish are not uncommon in the overlying 60 m of sediment, but the only evidence for benthic life are occasional bedding planes covered with a few species of bivalve, notably *Claraia*, and five beds with small, rare *Planolites* burrows (Fig. 1). This meager evidence for benthic colonization implies that benthic life was inhibited in the lower Vardebukta Formation. The fine lamination, presence of pyrite, and well-preserved (nonscavenged) fish are all suggestive of bottom-water anoxia. The onset of anoxic conditions is not coincident with the deepest water facies recorded at the base of the Vardebukta Formation; rather, it occurs during the subsequent aggradation within the basal parasequence. The return of normal, bioturbated aerobic biofacies (II 6) occurs near the top of a later parasequence in a sandstone at a level high in the Griesbachian Stage (Fig. 1).

The Spitsbergen data imply that anoxic conditions affected the boreal seas during the P-Tr crisis. In the western Tethyan sections of northern Italy, where the event was first recognized, the problems are different. The carbonate-dominated P-Tr succession of the Dolomites record a spectrum of depositional environments. The Permian Bellerophon Formation is disconformably overlain by the Werfen Formation, which, at its base, contains thin, strongly retrogradational oolite-bearing rocks, the Tesero Oolite horizon (TOH). The TOH is overlain by the Mazzin Member, which consists of thin, distal tempestites and laminated micrite. The first *H. parvus*, and therefore the base of the Triassic, is in the lower part of the Mazzin (*11*). On the margins of the basin, the Mazzin Member passes upward into the Andraz horizon, a peritidal unit, but more distally it is overlain by open marine carbonates of the Siusi Formation.

If the laminated and pyritic micrites of the Mazzin Member are interpreted as evidence of deposition under anoxic bottom waters (*2*), then the onset of anoxia was at a level similar to that seen in Spitsbergen. This interpretation is not accepted by all, however, and these sediments have been alternatively interpreted as supratidal flat facies (*12*). Geochemical evidence from the Mazzin Member of the Gartnerkofel-1 core (southern Austria), a location within the same depositional basin as the Italian outcrops, is more characteristic of anoxic deep water (*13, 14*). However, the Gartnerkofel-1 core samples more distal rocks, so perhaps this is not surprising. It has even been suggested that the generally laminated nature of the Early Triassic sedimentary rocks is caused by the paucity of a burrowing fauna in the aftermath of the extinction and not by any environmental changes (*1*).

To independently evaluate the redox conditions under which the Early Triassic sediments of northern Italy accumulated, we used gamma ray spectrometry; gamma rays of characteristic energy emitted during the radioactive decay of potassium, thorium, and uranium species are detected by a spectrometer. The ratio of Th/U calculated from the data can be used to estimate redox conditions in the depositional environment (*15*). In anoxic conditions, uranium is reduced to the insoluble uranous (U^{4+}) fluoride complex and can be preserved in the sediment, whereas in oxidizing environments, it is converted to a soluble uranyl (U^{6+}) carbonate, which is removed in solution. Anoxic sediments are therefore typically much more U-rich than oxic ones. Thorium is unaffected by redox conditions and remains in an insoluble state (Th^{4+}). The result is that anoxic sediments have Th/U ratios below 2, oxic marine sediments have ratios between 2 and 7, and intensely oxidizing terrestrial environments have ratios in excess of 7 (*15*). We made measurements over 3-min intervals and regularly repeated analyses. Errors on Th/U ratios were ±5% or less.

We measured eight sections over a total of 750 m of strata from the basal TOH to the top of the Siusi Member (Fig. 2). Facies analysis of the TOH suggests that it was deposited in well-oxygenated conditions. The amount of U detected in the dolomitized oolites was too low (less than 1.8 parts per million) to obtain a reliable signal, although as mentioned above, low U values are only to be expected in oxygenated facies. In contrast, the first development of Mazzin micrites is marked by a sharp swing to anoxic Th/U ratios. These facies are just above the last appearance of a moderately diverse Permian brachiopod, calcareous algae, echinoderm, and foraminiferan assemblage (*16*).

The data show that anoxia prevailed for much of the Mazzin depositional interval even in shallow ramp settings. Narrow intervals of slightly oxygenated conditions are seen from the mid-Mazzin upward in association with major storm beds [for example, at Bulla (Fig. 2)], indicating that occasional storms were able to oxygenate the benthic environment. However, most sections show no evidence for benthic oxygenation until the Andraz horizon, although some, such as the Medvodje section (Fig. 2), show a trend of increasing Th/U ratios up through the Mazzin. The evidence shows that anoxic bottom waters were present throughout the Mazzin interval in water depths above the storm wave base. The Andraz has Th/U ratios significantly greater than 2, suggesting oxygenated conditions. This result is to be expected considering the peritidal nature of the deposit. The upward passage from the anoxic ratios below occurs in as little as 1 m. It would appear that throughout much of its depth, the Mazzin sea was anoxic to dysoxic, and only in a narrow, peritidal fringing zone (separating supratidal flat from storm-dominated ramp facies) was the benthic environment oxygenated.

Anoxic ratios return abruptly in the micrites and wackestones at the base of the Siusi Member but only for a short interval (about 10 m), and normal marine ratios are rapidly established (Fig. 2) along with a burrowing fauna (II 3 through 5) and a modest diversity of shelly invertebrates (*17*). The Dolomites succession thus is similar to that of Spitsbergen; the anoxic event began late in the Changxingian, terminated late in the Griesbachian, and in both areas its effects can be detected in shallow marine settings subject to storm deposition.

The rapid demise of the Permian assemblages in the Dolomites is closely related to the development of dysaerobic facies, but diversity in the underlying few meters of strata is difficult to assess because of the dolomitization and recrystallization (*2, 12*). It is therefore difficult to directly equate the extinction and the onset of anoxic deposition. In South China, however, the relation is much clearer. The transition from the Permian to the Triassic is marked by the development of a remarkably uniform facies consisting of various proportions of thinly bedded marls and micritic limestones (*18*). The abundance of trace metal–enriched framboidal pyrite and fine lamination implies that the rocks were deposited in a low-oxygen environment (*19*). The demise of a high-diversity latest Changxingian benthic fauna (species diversities are commonly in the hundreds) generally occurs in the meter or so beneath the basal Triassic facies and is marked by a decline in the size, depth, and density of burrows (II 6 declining to 2 or 1) and the development of first pyrite steinkerns and then disseminated framboidal pyrite. The evidence points to a rapid development of anoxic depositional conditions through a succession of dysaerobic biofacies. In many sections, a mixed fauna of Permian brachiopods and Triassic bivalves, conodonts, and ammonoids occurs in a 10- to 30-cm-thick bed at the base of the Triassic. This transition bed records slightly dysoxic conditions: steinkern pyrite, low diversity, and small burrows (*2, 20*), a last gasp before the final suffocation.

The marine extinction mechanism thus appears to be closely related to the development of oxygen-restricted deposition, but the relation with the Siberian flood basalt eruptions and terrestrial extinctions requires thought. One notion is that the Siberian eruptions emitted CO_2 and other gases leading to global warming (*1, 21*). Sedimentological and paleobotanical evidence indicates rapid warming and the demise of cold-loving plants at the time of the mass extinction (*13, 22*). In the Early Triassic, warm, arid to semiarid conditions dominated over much of the equatorial and mid-paleolatitudes of Pangea, whereas the highest paleolatitudes only experienced a wet, temperate climate (*13, 22*). A remarkably cosmopolitan terrestrial fauna developed, testimony to a minimum of environmental heterogeneity. Temperature increase in the sea is unlikely to have caused extinction, unless the temperature considerably exceeded 30°C, an unlikely proposition, at least in mid to higher latitudes. A more direct cause of death may come from a double-edged effect of temperature rise: oxygen uptake of organisms rapidly increases with temperature rise, and yet oxygen solubility declines in warmer waters (*23*). However, probably the single most important cause of oxygen-deficient waters (and thus the marine extinction) was the decline in oceanic circulation as the equator-to-pole temperature gradient declined. Evidence from Japanese pelagic sediments indicate that the oceans began to stagnate in the Changxingian (*24*), precisely the time of the biotic crisis.

A rapid negative carbon isotope swing has been detected in carbonates and organic carbon from a number of P-Tr sections scattered throughout the world (*25*), implying a drop in productivity. However, $\delta^{13}C$ values rapidly increased a short distance above the P-Tr boundary, implying a recovery of productivity levels. Basal Triassic marine palynological assemblages are also characterized by prolific numbers

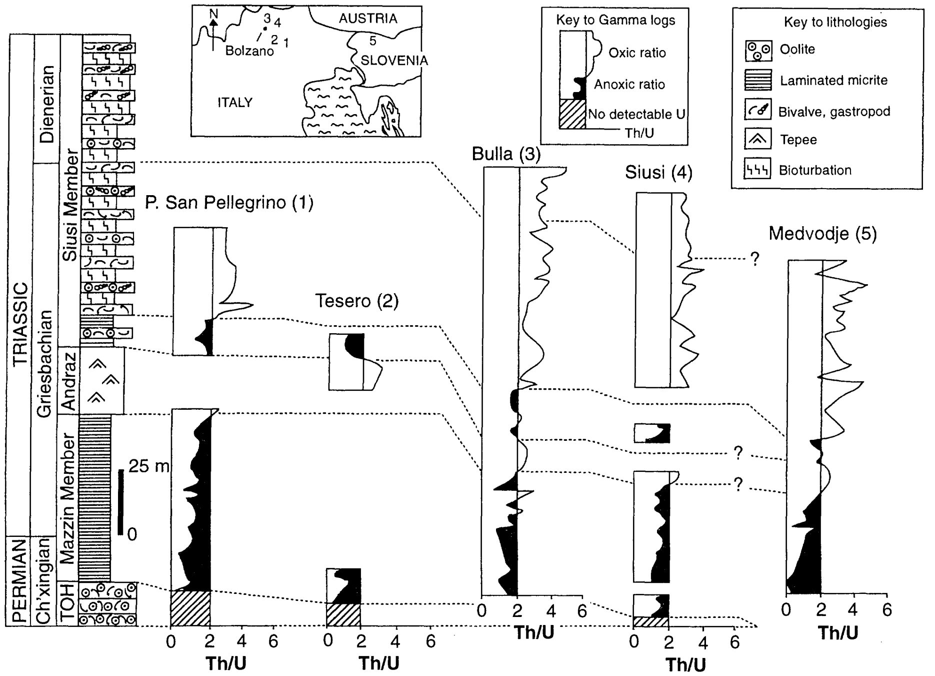

Fig. 2. Th/U ratios for several sections spanning the boundary of the Bellerophon and Werfen formations in the Dolomites (Italy) and Slovenia. The left to right (west to east) order of the sections records a transect from marginal localities in the west to more basinal localities in the east. Thus, the Andraz horizon, the most proximal, peritidal facies with tepees, is not seen in the most easterly Medvodje section of Slovenia. Anoxic ratios (less than 2) characterize much of the Mazzin Member and the basal meters of the Siusi Member and indicate that anoxic conditions affected all but the peritidal conditions of the Andraz in the early Griesbachian seas of this equatorial western Tethyan region.

of acritarchs, a sign of eutrophic conditions (*26*). Productivity crash followed by productivity boom is a characteristic of oceans in which a rapid decline of circulation rates produces an anoxic lower water column (*27*). Modeling shows that, initially, the productivity declines concomitantly with the decrease of the rate of oceanic overturn and nutrient supply. This effect is counterbalanced by the increased availability of reactive phosphorus (the principal biolimiting nutrient), which is not as efficiently sequestered by iron oxides and organic matter in an anoxic ocean. There is, however, a significant lag time (of the order of tens of thousands of years) between the onset of oceanic anoxia and the build-up of phosphorus (*27*), a delay that is disastrous for the marine biota.

REFERENCES AND NOTES

1. D. H. Erwin, *The Great Paleozoic Crisis* (Columbia Univ. Press, New York, 1993).
2. P. B. Wignall and A. Hallam, *Palaeogeogr. Palaeoclimatol. Palaeoecol.* **93**, 21 (1992).
3. ———, *ibid.* **102**, 215 (1993).
4. Jin Y., Zhu Z., Mei S., *Palaeoworld* **4**, 138 (1994); S. M. Stanley and X. Yang, *Science* **266**, 1340 (1994).
5. P. R. Renne, Zhang Z., M. A. Richards, M. T. Black, A. R. Basu, *Science* **269**, 1413 (1995).
6. A. Hallam, *Hist. Biol.* **5**, 257 (1991); *Can. Soc. Pet. Geol. Mem.* **17**, 797 (1994).
7. M. Gruszczynski, S. Halas, A. Hoffman, K. Malkowski, *Nature* **337**, 64 (1989).
8. K. Nakazawa, K. Nakamura, G. Kimura, *Proc. Jpn. Acad. Sci. B* **63**, 171 (1987); T. Ishibashi and K. Nakazawa, *Mem. Fac. Sci. Kyushu Univ. Ser. D* **26**, 215 (1989).
9. Yin H., Yang F., Zhang K., Yang W., *Mem. Soc. Geol. Ital.* **34**, 329 (1988); H. Kozur, *Zentralbl. Geol. Palaeontol. Teil 1* **11–12**, 1245 (1989); Ding M., in *Permo-Triassic Events in the Eastern Tethys*, W. C Sweet, Z. Yang, J. M. Dickins, H. Yin, Eds. (Cambridge Univ. Press, Cambridge, 1992), pp. 109–119; R. K. Paull and R. A. Paull, *Lethaia* **27**, 271 (1994). An unavoidable consequence of this otherwise commendable choice of P-Tr boundary is that the earliest part of the Griesbachian Stage (defined by the presence of *Otoceras* ammonoids), generally considered to be a basal Triassic age, becomes Permian in age.
10. M. L. Droser and D. J. Bottjer, *J. Sediment. Petrol.* **56**, 558 (1986).
11. P. B. Wignall, H. Kozur, A. Hallam, *Hist. Biol.*, in press.
12. S. U. Noé, *Facies* **16**, 89 (1987); ——— and W. Buggisch, *Jahrb. Geol. Bundesanst. Wien* **137**, 297 (1994).
13. W. T. Holser, H. P. Schönlaub, K. Boeckelmann, M. Magaritz, C. J. Orth, *Abh. Geol. Bundesanst. Wien* **45**, 213 (1991).
14. The evidence includes light pyrite sulfur isotopes diagnostic of syngenetic or early diagenetic formation and trace metal enrichment (V and Ni) typical of black shale environments. One of us (R.J.T.) has examined the core material and found that the Mazzin Member is finely laminated throughout and devoid of the indicators of a supratidal flat (for example, tepees and fenestrae). However, it could be argued that the more distal, basinal setting of the Gartnerkofel site makes it a poor comparison with the generally more proximal localities of the Dolomites, hence the essential need for independent geochemical corroboration from the latter region.
15. J. A. S. Adams and C. E. Weaver, *Am. Assoc. Pet. Geol. Bull.* **42**, 387 (1958); F. B. Zelt, *Soc. Econ. Pal. Min. Field Trip Guidebook* **4**, 49 (1985); K. J. Myers and P. B. Wignall, in *Marine Clastic Environments: New Concepts and Case Studies*, J. K. Legget and G. G. Zuffa, Eds. (Graham and Trotman, London, 1987).
16. C. Broglio Loriga, C. Neri, M. Pasini, R. Posenato, *Mem. Soc. Geol. Ital.* **34**, 5 (1988).
17. R. J. Twitchett and P. B. Wignall, *Palaeogeogr. Palaeoclimatol. Palaeoecol.*, in press.
18. Yang Z. and Li Z., in *Permo-Triassic Events in the Eastern Tethys*, W. C. Sweet, Yang Z., J. M. Dickins, Yin H., Eds. (Cambridge Univ. Press, Cambridge, 1992), pp. 9–20.
19. He J., *Hist. Biol.* **2**, 73 (1989); P. B. Wignall, A. Hallam, Lai X., Yang F., *ibid.* **10**, 175 (1995); P. B. Wignall and A. Hallam, *Palaios*, in press.
20. D. J. Bottjer, M. L. Droser, Wang C., *Geol. Soc. Am. Abstr. Programs* **20**, A106 (1988)
21. R. Brandner, *Ber. Geol. Bund. Wien* **15**, 3 (1988); J. J. Veevers, P. J. Conaghan, S. E. Shaw, *Geol. Soc. Am. Spec. Pap.* **288**, 187 (1994).
22. S. V. Meyen, *Can. Soc. Pet. Geol. Mem.* **2**, 662 (1973); I. A. Dobruskina, *Palaeogeogr. Palaeoclimatol. Palaeoecol.* **58**, 75 (1987); G. Retallack, in *International Geology Congress in Beijing: Abstracts Volume* (in press). The eclectic evidence includes oxygen isotope, fossil plant, and paleosol data.
23. P. W. Hochachka and G. N. Somero, *Biochemical Adaptation* (Princeton Univ. Press, Princeton, NJ, 1984). A 10°C temperature increase doubles the rates of physiological reactions and consequent oxygen requirements.
24. Y. Isozaki, *Can. Soc. Pet. Geol. Mem.* **17**, 805 (1994).
25. M. Magaritz, R. V. Krishnamurthy, W. T. Holser, *Am. J. Sci.* **292**, 727 (1992); K. Wang, H. H. J. Geldsetzer, H. R. Krouse, *Geology* **22**, 580 (1994).
26. B. E. Balme, *Univ. Kansas Spec. Publ.* **4**, 305 (1970); G. J. Retallack, *Science* **267**, 77 (1995).
27. E. D. Ingall, R. M. Bustin, P. van Cappellen, *Geochim. Cosmochim. Acta* **56**, 3323 (1993); P. van Cappellen and E. D. Ingall, *Paleoceanography* **9**, 677 (1994).
28. The Spitsbergen fieldwork was supported by a grant from the Royal Society and the Cambridge Arctic Shelf Programme. The Dolomites fieldwork was supported by a Natural Environment Research Council postgraduate studentship.

16 January 1996; accepted 21 March 1996

Nanotribology and Nanofabrication of MoO_3 Structures by Atomic Force Microscopy

Paul E. Sheehan and Charles M. Lieber*

Atomic force microscopy was used to characterize the sliding of molybdenum oxide (MoO_3) nanocrystals on single-crystal molybdenum disulfide (MoS_2) surfaces. Highly anisotropic friction was observed whereby MoO_3 nanocrystals moved only along specific directions of the MoS_2 surface lattice. The energy per unit area to move the MoO_3 nanocrystals along their preferred sliding direction was an order of magnitude less than required to slide macroscopic MoS_2-bearing contacts. This extreme friction anisotropy was exploited to fabricate multicomponent MoO_3 nanostructures. These reversibly interlocking structures could serve as the basis for devices such as mechanical logic gates.

Three centuries of macroscopic studies of friction, adhesion, and wear have contributed much to the phenomenological understanding of tribology (*1*, *2*). However, studies of interactions between macroscopic bodies are influenced by complex factors, including surface roughness and adsorbates, that have precluded the development of a first-principles understanding of friction and adhesion (*2*, *3*). In principle, nanometer-scale measurements of friction and adhesion forces should be interpretable in terms of fundamental intermolecular forces, and such measurements could thus play a central role in the development of microscopic models of friction and the rational design of improved lubricants. Moreover, such microscopic information is highly relevant to the emerging field of nanotechnology, where noncovalent interactions are important in the manipulation, assembly, and stability of new structures.

Atomic force microscopy (AFM) can be used to measure normal (adhesive) and lateral (friction) forces on the nanometer scale, and thus it is a powerful technique for probing the microscopic mechanism of friction (*3*–*8*). Studies of friction between probe tips and different surfaces have yielded a number of interesting observations, including atomic scale stick-slip motion (*4*, *6*) and functional-group dependence of friction (*7*, *8*). These studies have also raised the issues of whether friction depends on the crystallographic direction of sliding and whether the contact between an AFM microscope probe tip and a surface is a single- or multiple-asperity contact (*9*, *10*).

These issues highlight a principal weakness of AFM for tribology: The structure of the probe tip–sample sliding interface may not be well defined, even though the probe tip can provide nanometer-scale resolution. Here, we eliminated this essential uncertainty by probing the friction of MoO_3 nanocrystals sliding on single-crystal MoS_2. This system is well suited for nanotribology studies because the interface structure and contact area are atomically defined and because the MoO_3

Department of Chemistry and Division of Applied Sciences, Harvard University, Cambridge, MA 02138, USA.

*To whom correspondence should be addressed.